

UNIVERSIDAD CARLOS III DE MADRID
SCHOOL OF GRADUATE STUDIES
BIOENGINEERING AND AEROSPACE ENGINEERING DEPARTMENT



MASTER IN SPACE ENGINEERING

MiSE

Title: Launch Vehicle Interstage Structure Design

Author:
Carlos Quintana Gómez

Tutor:
Víctor Bautista Juzgado

Course 2023/2024

Contents

Acronyms	3
1 Introduction	4
1.1 Launch vehicles and their components	4
1.2 Case Study	5
2 Data Exchange and Deliverables	6
3 Fundamentals of interstage structures in launch vehicle design	8
3.1 Definition and function of interstage structures	8
3.2 Structural requirements and challenges	10
3.2.1 Mission Requirements	10
3.2.1.1 Ground and Test Loads	11
3.2.1.2 Launch Loads	11
3.2.2 Functionality Requirements	12
3.2.3 Interface Requirements	13
3.2.4 Design Requirements	13
3.2.5 Verification Requirements	13
3.3 Material selection and design concept considerations	14
3.3.1 Aluminum case	15
3.3.2 Honeycomb case	16
4 Motivation & Objectives	17
5 Hands-On development Design and analysis	18
5.1 QSL Envelope of Ariane 5	18
5.2 Aluminum interstage structure	19
5.2.1 Aluminum QSL Analysis	22
5.2.1.1 Upper stage axial and shear stress contribution	23
5.2.1.2 Bending moment launcher contribution	26
5.2.2 Aluminum QSL Results	27
5.2.3 Aluminum Buckling Analysis	28
5.2.4 Aluminum Buckling Results	29
5.3 Honeycomb Interstage Structure	30
5.3.1 Honeycomb QSL and Buckling Analysis	30
5.3.2 Honeycomb QSL Results	32
5.3.3 Honeycomb Buckling Results	33
6 Design	34
6.1 Challenges	34
6.2 Failure Modes	34
6.2.1 System level failure modes	34
6.3 Requirements analysis and mission profile considerations	34
6.4 Conceptual design phase	34

7 Mechanical Environments	35
7.1 Structural loads and their effects?	35
7.2 Detailed design phase	35
7.3 Structural analysis and optimization techniques	35
8 Finite element description. Finite Element Analysis (FEA) techniques	35
9 Structural Analysis	35
9.1 Static Analysis	35
9.2 Buckling Analysis	35
9.3 Stress analysis and failure modes?	35
10 Manufacturing and Testing	35
10.1 Manufacturing techniques for interstage structures	36
10.2 Non-destructive testing methods	36
10.3 Full-scale testing and validation	36
11 Performance Evaluation	36
11.1 Comparative analysis of the designed interstage structure with existing ones	36
11.2 Evaluation of performance metrics such as weight, stiffness, and reliability	36
12 Future Developments and Challenges?	36
12.1 Emerging trends in launch vehicle design	36
12.2 Potential improvements in interstage structures	36
12.3 Challenges and areas for future research	36
13 Conclusion	36
14 References	36

Acronyms

CASA Construcciones Aeronáuticas SA

CFE Critical Flight Event

CFRP Carbon Fiber-Reinforced Plastic

ISS INTERSTAGE SKIRT STRUCTURE

MoS Margin of Safety

QSL Quasi-Static Load

SPC Single Point Constraint

1 Introduction

1.1 Launch vehicles and their components

A launch vehicle is a vehicle that is propelled by a rocket engine to carry payloads to orbit. These payloads can be manned spacecraft or satellites. The term launch vehicle is more general because it includes ballistic missiles, rockets, the Space Shuttle, etc. These launch vehicles are complex and are composed of several systems that work together to accomplish a mission. More about this definition in reference [18].

These systems can be grouped into four major systems, the Structure, the Propulsion, the GNC and the Payload systems, as we can see in Figure 1. The Propulsion is the system responsible for providing the thrust and speed necessary to move the launcher. This system is supported and sustained by the Structure system, which carries all the systems, including the rocket's fuel and engines. The propulsion cannot function without the GNC system, which is the brain that leads the rocket to the desired orbit, which is where the mission normally ends, putting the payload into the desired route.

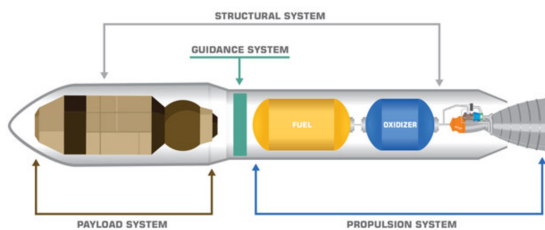


Figure 1: 4 main systems of a launch vehicle, [14].

Focusing on the structural system, it has to be strong enough to withstand all the launch forces, but it also has to be light enough to allow for easier and less costly orbiting. As the structure has to be as light as possible, materials such as titanium, aluminum and [Carbon Fiber-Reinforced Plastic \(CFRP\)](#) are often used to build the largest and most critical parts of a rocket, which will be discussed in more detail in subsection 3.3.

Therefore, from the structural perspective, launch vehicles are composed of various components designed to withstand the immense forces and harsh environments encountered during launch. The main parts can be classified as follows:

- Fuselage or Body
- Rocket Stages
- Tankage
- Interstage Structures
- Payload Adapter
- Fairings

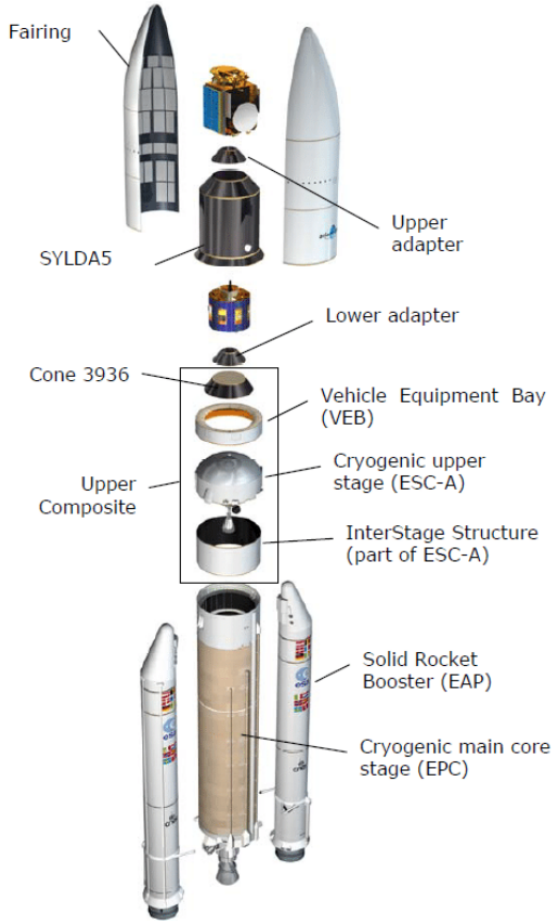


Figure 2: Launch vehicle general data [1].

This project delves into the essential principles necessary for developing a structural component of a launcher. Specifically, these principles are applied to a particular case study to outline the design, analysis, and manufacturing processes of an interstage structure. The thesis also details my personal approach to designing and analyzing this case, as my aim was to learn and improve existing practices through this specific project.

1.2 Case Study

This work analyzes the interstage structure of the Ariane 5 rocket. Rather than studying the original structure in detail, the focus is on creating an imitation or improvement. This approach facilitates an understanding of the design and preliminary decisions required to develop a structure that meets specifications. Simplifications are implemented to clarify the design decisions and are explained throughout the project.

Before choosing to focus on the Ariane 5 interstage structure, various interstage structures from other launchers were examined. Vented structures from the Soyuz and Starship designs were considered, as well as non-vented interstage structures from the Saturn V, Atlas V, and Falcon 9 rockets.

However, my primary interest lies in European launchers like the Ariane 5 and Ariane 6. Studying these European rockets provides better insight into the context in which I am likely to work, enhancing my skills for the future.

Notably, both the Ariane 5 and Ariane 6 interstage structures were developed by Airbus Spain ([Construcciones Aeronáuticas SA \(CASA\)](#)), as illustrated in [Figure 3](#) and [Figure 4](#). My master's thesis tutor, Víctor Bautista Juzgado, has worked for Airbus Space and Defense and participated in the Ariane 5 interstage structure, providing invaluable guidance throughout this work. Additionally, at my current workplace, Capgemini Engineering has supported the design and analysis of the Ariane 6 interstage structure in collaboration with Airbus, with colleagues who participated in this project offering their assistance. I would like to thank Victor Bautista and Capgemini Engineering for their support and knowledge, which have been instrumental during these months of work.

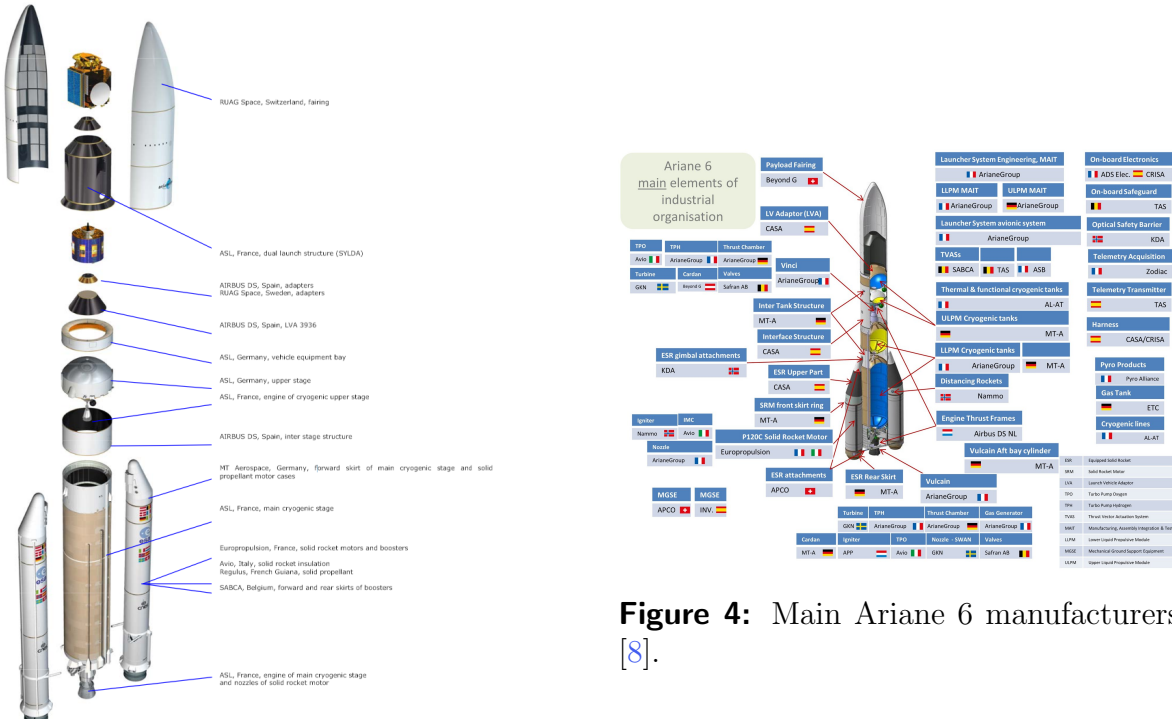


Figure 3: Main Ariane 5 manufacturers [\[1\]](#).

2 Data Exchange and Deliverables

All the work is shared on GitHub, including the 3D CATPart and CATProduct models (CATIA V5), as well as the .h HyperMesh, .bdf models, and .dat files. Everything is organized for each type of analysis. Feel free to review it.

For an actual project, the necessary data exchange would involve the following steps:

- Geometrical data exchanged between CAD and CAE software tools (Done).

- Data exchange between structural design and manufacturing (Done just .design part).
- Data exchange with other subsystems (Not done for this project).
- Structural analysis and tests (Done just analysis).
- Structural mathematical models (FEM section).

In terms of deliverables for inter-stage structures, the typical items include.

- Computer aided design (CAD) model description (Done).
- Design loads documentation (Done).
- Dimensional stability analysis (Done).
- Buckling analysis results (Done).
- Fatigue analysis.
- Fracture control analysis or plan.
- Description of the Mathematical model (Finite Element Method - FEM) (Done).
- Analysis of modal and dynamic responses.
- Stress and strength analysis report (Done).
- Structure alignment budget details.
- Summary of structure mass (pending).
- Prediction of test outcomes (pending).
- Correlation between test results and analysis.

From this list, we will prioritize the most relevant ones for our specific case.

3 Fundamentals of interstage structures in launch vehicle design

A rocket interstage structure is nothing more than a cylindrical structure that connects two stages of a launcher, usually made of strong and lightweight materials such as aluminum and/or CFRP.

The following explains in more depth the importance of an interstage structure, what it is, and why it plays a crucial role in an orbital launcher.

3.1 Definition and function of interstage structures

The diameter of a interstage structure is adapted to the dimensions of the stages it is joining. Therefore, some structures have an uniform cylindrical shape and others have conical reductions for upper stage adaption as can be seen in the following [Figure 5](#) and [Figure 6](#) respectively.



Figure 5: Ariane 5 Plus - Inter Stage Structure [\[6\]](#).



Figure 6: Vega-C 1/2 interstage integration CSG [\[9\]](#).

Similarly, the length of an interstage varies depending on factors such as the stresses it supports, mechanisms and other systems it must contain but, above all, the extension of the upper stage nozzle it has to contain. This brings to the table the most important and main function of an rocket interstage structure, which is to provide space between stages.

However, this is not its only function. The most important objectives of an interstage structure are presented below:

1. **Secure clamping and stage separation.**

It seems obvious, but an interstage structure ensures the separation of two stages when it is foreseen. This separation can be done in different ways depending on the launcher. The interstage structure can be separated from both stages in a specific sequence or

it can be separated from only one of them. Two popular cases are explained in this section.

2. Space between stages.

interstage spacing is required to contain the necessary components. The main components are the upper stage nozzle, mechanisms, and all systems needed for the structure to fulfill its task. This space is given for safety reasons which are explained below.

3. Upper stage nozzle protection.

Conceptually speaking and not in all cases, the interstage structure that fills the interstage gap is not there just to create space to fit the nozzle and other components (this could be integrated in the lower or upper stage and problem solved), but the real reason behind it is that it provides protection. The most obvious and relevant protection is to prevent a collision between the first stage and the nozzle at stage separation.

The stage separation of a Saturn V occurs in a specific sequence in which the first stage is ejected first. Then, after a few seconds, the interstage structure pushes the upper stage with small thrusters to prevent sloshing. The interstage structure is then ejected from the second stage to save weight. A different case is Falcon 9, where the interstage structure is integrated into the first stage. It therefore remains attached to the first stage due to the reusable nature of the launcher. Thus, nozzle protection is provided by controlled stage separation with a pneumatic release system using multiple Helium-actuated hydraulic pistons.

4. Avoid sloshing.

One of the most critical moments of a launch is the stage separation and one of the main risks during this operation is sloshing. Sloshing is an effect that occurs after the shutdown of the lower stage engines, which causes an abrupt stop in the rocket's acceleration. This abrupt change causes a period of weightlessness, which can lead to separation of the liquid propellants from the bottom of the upper stage tanks causing bubbles and cavitation, which can be absorbed by the upper stage engines when activated. If this occurs, the most likely result is a "Rapid Unscheduled Disassembly". Sloshing is the main reason SpaceX has gone with the hot-staging separation method for its Starship/Super Heavy prototype.

Hot staging is an old and popular solution created for the Soviet/Russian rocket family, which consists of starting the second stage engines when the first stage engines are still running but about to shut down. This can be achieved by a vented structure that allows exhaust gases to escape without causing overpressure, explained below. Another popular solution, as on the Saturn V, is the use of ullage thrusters located in the interstage structure, which are activated after separation to provide this acceleration to settle the propellants where they need to be as explained above. Once the function of this structure has been fulfilled, it is ejected to save mass.

5. Protect against rapid pressure increase in the space-optimized rocket motor.

In many cases, after first stage separation, a safety distance is usually expected between the upper and lower stages to avoid unnecessary overpressure of the exhaust gases.

This is usually a factor to be considered in the case of hot-staging, as there is a risk of damaging or even destroying the nozzle and/or the combustion chamber. For this reason, in a hot-staging separation, the interstage structure has to be “vented”.

3.2 Structural requirements and challenges

Properly defining all the requirements is crucial for effective design. Everything begins with clear requirements, and they should guide the entire process. For instance, if a mission requirement states, “It cannot weigh more than 300kg,” this will lead to a structural requirement like “The structure should be made of CFRP” to meet the mission’s needs.

Weight is a critical component in space because every kilogram adds a high energy cost in the form of propellant. This leads to larger fuel tanks, heavier structures, and ultimately, even more fuel—creating a Catch-22 situation. Consequently, safety margins in space are kept low to address these challenges. A [Margin of Safety \(MoS\)](#), as shown in the following [Equation 1](#), is defined as the ratio of a material’s yield stress to the applied stress, minus 1. If the MoS is greater than 1, it means the applied stress is lower than the yield stress. Therefore, it is essential for safety margins to be greater than one to prevent failure. For space structures, safety margins typically range between 1.2 and 1.5, [3]. [CFRP](#) is often used for its high E/ρ ratio (Young’s modulus over density) and dimensional stability, as explained in the “Materials” section.

$$MoS = \frac{\sigma_{allowable}}{\sigma_{applied} \cdot SF} - 1 \quad (1)$$

In summary, the typical properties of a launch vehicle include:

- High strength
- Low mass (to increase payload capacity)
- Pressurized compartments (except for interstage structures)

Everything starts with a requirement. A mission requirement leads to a structural requirement, such as ”the structure should be made of CFRP”. Therefore, the goal is to define all requirements related to the structure, including specification, design, development, verification, production, and in-service use. Maintaining a balance between subsystem requirements is crucial throughout the entire mission project. This section focuses on the typical and general requirements for an interstage structure.

3.2.1 Mission Requirements

The mission requirements of a interstage structure shall take into account the expected events that the structure suffers during its lifetime and during its natural and induced environments.

For the lifetime events the structure shall withstand first transportation, handling, testing and storage. A secondly shall withstand all phases of pre-launch, launch and operation.

For the structure natural and induced environments, development shall consider on ground, launch and operational environment conditions. This includes for example atmospheric conditions in which they are manufactured, stored and tested, including corrosion effects.

So basically the launcher structure mechanical environments can be divided into static, thermal and dynamic loads. Normally, for spacecraft structures Static and dynamic environment loads shall be defined in terms of constant acceleration, transient, sinusoidal and random vibration, acoustic noise and shock loads shall be used in the worst combinations in which they can occur. It is important to note that for this master thesis, as the case of study is a interstage structure, it is not possible to perform most of the tests at launcher level (physical constraints). Typically these tests are Static Tests (set-up with auxiliary structures, hydraulic jacks...). This is not a problem because static loads covers the spectrum of dynamic loads.

However, for our case it is very important to consider load events, that is, stage separation. “Different load cases that appear during the whole structure lifetime”

Since the actual launcher specifications are not available, the specifications from the user’s manual were used instead. These specifications reflect the conditions a payload experiences when being launched into orbit. Although they might not be entirely accurate, they are sufficient for an initial sizing of the structure. The goal is to simplify the dimensioning process and demonstrate the development methodology. The loads specified in the Ariane 5 user’s manual include inherent safety margins. An additional safety factor of 1.25 (qualification), as recommended in the manual, will be applied to these loads for the preliminary design. In a real scenario, this approach can be replicated using the actual specifications. The process will be detailed further in the ”development” section.

The following are the types of load events that a structural part, such as an interstage, must be able to withstand and to which it must be analyzed and tested. This is explained here for theoretical purposes.

3.2.1.1 Ground and Test Loads

- Handling, transportation and storage loads
- Assembly and integration loads
- Ground test loads

3.2.1.2 Launch Loads

- Launch preparation
- Operational pressures
- Engine ignition
- Thrust built-up

- Aborted launch
- Lift-off
- Thrust (constant or varying slowly)
- Aerodynamic loads
- heat flux from engine and aerodynamics
- Wind and gust
- Dynamic interaction between the structure and propulsion system
- Thrust decay
- Acoustic noise
- Pyrotechnics
- Separation of parts (e.g. stage, interstage, fairing and spacecraft)

For mission requirements do we have to consider combined loads? I.e. linear combination, root of squaresum Load application sequence (non-linear)

Limit loads. Load level not being exceeded with a probability of 99 % and a confidence level of 90 percent during the service-life

Design limit loads. Multiplication of the limit loads by the design factors

DLL = LL x DF Limit loads per Design Factor

3.2.2 Functionality Requirements

Structural parts must meet specific functional requirements to ensure they can withstand various loads without issues. The necessary capacities include:

- Strength: Ability to withstand loads without rupturing.
- Yielding: Ability to endure loads without permanent (plastic) deformation.
- Buckling: Ability to resist compression loads without instability.
- Stiffness: Ability to bear loads without excessive deformation, measured by Young's modulus $E = \sigma/\epsilon$
- Dynamic behavior: Ability to withstand dynamic loads.
- Thermal resistance: Ability to endure thermal loads.
- Damage tolerance: Ability to sustain defects (e.g., cracks).

3.2.3 Interface Requirements

Rocket interstage structures must be compatible with both internal and external interfaces. Internal interfaces include thermal control, mechanisms, propulsion, pyrotechnics, and materials. External interfaces involve the spacecraft-launcher interface, human factors, equipment, avionics, robotics, and ground support equipment (GSE), which encompasses all auxiliary equipment used on the ground.

The definition of these interfaces covers various aspects. Design aspects include areas, volumes, alignments, surface finishing, tolerances, geometry, flatness, fixations, mass, and inertias. Other considerations involve external loads (including temperature and thermal fluxes), global and local stiffness, and electrical and magnetic aspects.

3.2.4 Design Requirements

When designing interstage structures, several factors must be considered:

- Inspectability (NDI): Ensuring the ability to inspect components using Non-Destructive Inspection (NDI) methods.
- Interchangeability: Designing for the ease of interchanging components as needed.
- Maintainability: Ensuring the structure is easy to maintain for prolonged use.
- Dismountability: Designing for the capability to be disassembled when necessary.
- Mass and Inertia Properties: Understanding and managing mass and inertia properties to optimize performance.
- Material Selection (Corrosion): Selecting materials that are resistant to corrosion.
- Material Design Allowables: Determining allowable stresses (A-values) for chosen materials.
- Type of Materials: Considering various material types such as metals, non-metallic materials, glass and ceramics, composites, and adhesives.
- Margin of Safety (MoS): Ensuring all structural elements have a positive margin of safety.
- Factors of Safety (FoS): Typically set at 1.25 for qualification purposes, providing an additional safety margin.

3.2.5 Verification Requirements

Verification requirements have a specific order, contingent upon whether the design is new or not. Initially, analysis takes precedence, followed by testing, design review, and ultimately, the assessment of heritage or similarity.

This work underscores verification through analysis. The following encompasses the aspects typically taken into account for real verifications for rocket structures (not all apply to interstages): Modelling aspects, static analysis, modal analysis, dynamic response, acoustic analysis, fatigue analysis, fracture control, buckling, thermo-elastic and hygro-thermal effects, joint analysis (bonded, bolted, welded, riveted), inserts analysis, aeroelastic analysis, mass and inertia properties assessment, alignment verification, dimensional stability assessment, analysis of microvibrations, microgravity, audible noise, and human-induced vibration, model philosophy (including different approaches such as QM + PFM + FMs, Prototypical approach, and Hybrid approach), various testing procedures (development tests, qualification tests, acceptance tests, static tests, modal survey tests, dynamic tests, acoustic tests, fatigue and fracture tests, microvibration tests, non-destructive inspections, thermoelastic tests, thermal cycling tests, ageing tests, contamination tests, mass properties measurement, alignment checks, dimensional stability tests, geometrical control, interface verification, aeroelastic tests, and lightning protection verification).

3.3 Material selection and design concept considerations

In this project, both aluminum and composite materials have been considered, either independently or in combination. The composite section presents various structural design options, as illustrated in the following [Figure 7](#). While these options were evaluated for the interstage of the Ares V, it's recommended to review the associated paper for a thorough analysis, [13]. This paper provides a comprehensive comparison between design concepts and the number of frames chosen, along with explanations of preliminary design structural models. Additionally, it compares Honeycomb Sandwich Design versus Hat-Stiffened Design, analyzing the mass per square inch for each based on the number of frames (or rings), and presents the results and plots. In this particular case, a hat-stiffened design emerged as the most optimal solution.

1. Aluminum honeycomb core sandwich
2. Foam core sandwich
3. Fiber reinforced foam core sandwich
4. Uniaxially-stiffened skin (I-beam stiffeners)
5. Hat-stiffened skin
6. Corrugated sandwich

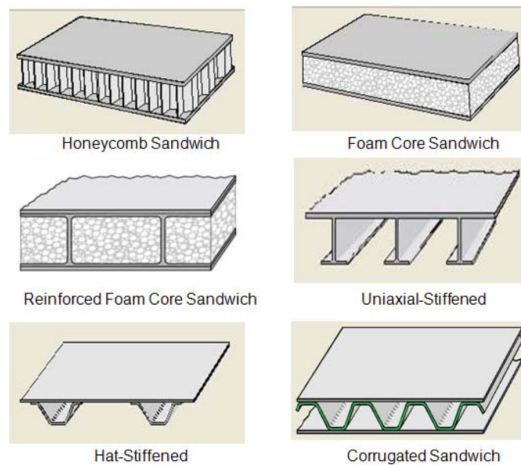


Figure 7: Design concept considerations, reference [13].

The interstage of the Ariane 5 utilizes Carbon Fiber Reinforced Polymer (CFRP) with a structural configuration of CFRP Sandwich with Aluminum Honeycomb. It also features lower and upper interfaces of aluminum rings riveted to the CFRP Sandwich. The manufacturing process involves Automatic Fiber Placement.

Given that the target emulation is the Ariane 5, the initial step involved attempting to create an interstage using solely aluminum, followed by a comparison with the actual structure. Subsequently, the next step was to replicate it with a honeycomb structure, mirroring the original design, and then compare it once more. Further details on this process are provided later on.

3.3.1 Aluminum case

For selecting the aluminum alloy for an interstage structure, it is essential to consider the specific requirements of aerospace applications. High strength-to-weight ratio is a primary criterion, but factors such as corrosion resistance, weldability, and manufacturability are also crucial.

Based on these criteria, the commonly used aluminum alloys in aerospace include 7075, 2024, 6061, and 7050. Each of these alloys are suitable for structural components in aerospace applications.

After consulting industry standards and typical aerospace applications, the following [Table 1](#) lists aluminum alloys that meet these criteria.

- 7075-T6 offers high strength and good fatigue resistance, but it has lower corrosion resistance and is not as weldable.
- 2024-T3 provides good strength and excellent fatigue resistance, with better machinability compared to 7075. However, it has poorer corrosion resistance.
- 6061-T6 has good strength and offers excellent corrosion resistance, as well as very good weldability and machinability. It has the lowest strength among the alloys listed.

Aluminum	Density (ρ) [kg/m^3]	Young's modulus (E) [MPa]	Yield strength (σ_t) [MPa]	Poisson's ratio (ν)
7075-T6	2810	71700	430-480	0.33
2024-T3	2780	73000	270-280	0.33
6061-T6	2700	68000	270	0.33
7050	2700	75000	455	0.33

Table 1: General properties of aluminum alloys, [16]

- 7050 is known for its high strength and excellent stress corrosion resistance, making it a popular choice in aerospace applications. It offers better corrosion resistance than 7075.

When comparing these alloys:

1. 7075-T6 and 7050 provide the highest strength.
2. 2024-T3 is chosen for its excellent fatigue resistance and machinability.
3. 6061-T6 offers the best corrosion resistance and weldability but has the lowest strength.

Given the requirement for a high strength-to-weight ratio in a rocket interstage structure, 7050 Aluminum Alloy stands out as the best choice. It balances high yield strength and tensile strength, slightly lower than 7075 but with significantly better corrosion resistance. However, if ultimate tensile strength is the most critical factor, 7075-T6 is also an excellent choice, though it would require additional corrosion protection measures.

3.3.2 Honeycomb case

For the second case, a sandwich structure with an aluminum core and CFRP skins has been selected. The following [Table 2](#) displaying typical values for a Carbon Fiber Reinforced Polymer (CFRP) used to define the material in the BDF. These values are commonly used in defining composite materials, such as CFRPs, in Finite Element Analysis (FEA) software. They are derived from material testing, engineering standards, and specifications provided by manufacturers or research institutions.

E_1	E_2	NU_{12}	G_{12}	$G_{1,Z}$	$G_{2,Z}$	RHO	A_1	A_2
200 GPa	10 GPa	0.3	8 GPa	6 GPa	6 GPa	1600 kg/m ³	1.0e-6 1/K	1.5e-6 1/K
$TREF$	X_t	X_c	Y_t	Y_c	S	GE	F_{12}	$STRN$
293.15 K	500 MPa	-500 MPa	400 MPa	-400 MPa	50 MPa	0.02	0.0	1.0

Table 2: Carbon Fiber Reinforced Polymer properties.

Being:

- E_1 Modulus of elasticity in longitudinal direction.

- E_2 Modulus of elasticity in lateral direction.
- ν_{12} Poisson's ratio (ϵ_2/ϵ_1).
- G_{12} Inplane shear modulus.
- $G_{1,Z}$ Transverse shear modulus for shear in 1-Z plane.
- $G_{2,Z}$ Transverse shear modulus for shear in 2-Z plane.
- ρ Mass density.
- α_1 Thermal expansion coefficient in 1-direction.
- α_2 Thermal expansion coefficient in 2-direction.
- T_{REF} Reference temperature for the calculation of thermal loads.
- X_t, X_c, Y_t, Y_c Allowable stresses or strains in the longitudinal and lateral directions.
Used for composite ply failure calculations.
- S Allowable for in-plane shear stresses or strains for composite ply failure calculations.
- GE Structural Element Damping Coefficient.
- F_{12} Tsai-Wu interaction term for composite failure.
- $STRN$ Indicates whether X_t , X_c , Y_t , Y_c , and S are stress or strain allowables.

Para disposicion preliminar elegida para la honeycomb es la siguiente. El espesor del core de 10mm y el espesor de cada ply de CFRP de 0.2mm. Aunque para un tipo de estructura igual es mejor desarrollar un material anisotropico, quizas dando mas rigidez en la z-direccion, se ha decidido hacer una configuración isotropica. Es por eso por lo que inicialmente se ha compuesto la skin con 4 plies rotadas de la siguiente forma 0/45/-45/90.

4 Motivation & Objectives

My primary motivation for this project has been to delve into the analysis of structural components in a broader context. It's been rewarding to apply this knowledge to a rocket's structural part, as this project aligns with my career aspirations in a specialized branch of engineering. Through this work, I have been able to utilize the expertise gained during the Master in Space Engineering at Carlos III University of Madrid.

During my year of working in the sector, my primary focus has been on design. However, I came to realize that I hadn't fully utilized my calculus knowledge. So, I actively pursued an opportunity to delve into this area, which has been incredibly valuable in clarifying concepts that were previously unclear to me. I'm grateful for the support of my tutor, Víctor Bautista Juzgado, and my coworkers of analysis at Capgemini Engineering.

Turning back to the project, the goal is to recreate the interstage of the Ariane 5 to investigate possibilities for reducing weight. It's important to recognize that certain simplifications were made during this process, meaning that the comparison might not be entirely fair. However, despite these limitations, this exercise has deepened my understanding of the analysis process within the context of a real-world project.

5 Hands-On development Design and analysis

This section provides a step-by-step explanation of the design and analysis process. It details the guidelines followed, the sources of the loads, and everything related to the overall procedure.

5.1 QSL Envelope of Ariane 5

The Ariane 5 User's Manual provides the following dimensioning loads, [Figure 8](#). It should be noted that these are the loads for sizing a payload to be launched on the Ariane 5. However, since the specifications of the launcher or those used for the Ariane 5 interstage structure are not available, the analysis has been conducted using these loads.

Acceleration (g) Critical flight events	Longitudinal		Lateral	Additional line load (N/mm)
	Static	Dynamic	Static + Dynamic	
Lift-off	- 1.8	\pm 1.5	\pm 2	26
Aerodynamic phase	- 2.7	\pm 0.5	\pm 2	23
Pressure oscillations / SRB end of flight	- 4.40	\pm 1.6	\pm 1	37
SRB jettisoning *	-0.7	\pm 3.2	\pm 0.9	0

Figure 8: Table 4.2.4.1.a – Quasi-Static Loads – Flight limit levels, [\[1\]](#).

These loads come with tolerances that create the most critical scenarios. Quasi-Static Loads are a combination of static and dynamic loads, as shown in the following [Figure 8](#), which lists the static and dynamic loads in the longitudinal and lateral directions. For lateral acceleration, the static and dynamic components are already combined, but this is not the case for the longitudinal direction. Therefore, for each [Critical Flight Event \(CFE\)](#), the load of the static component in the longitudinal direction is added to the dynamic component along with the tolerance. For example, the worst-case compression during Lift-Off would be -1.8g (static) - 1.5g (dynamic) = -3.3g . By making all the combinations of the four [CFEs](#), the [QSL envelope](#) can be obtained, [Figure 9](#). Note that in this plot, compression accelerations have been considered positive (negative in [Figure 8](#)).

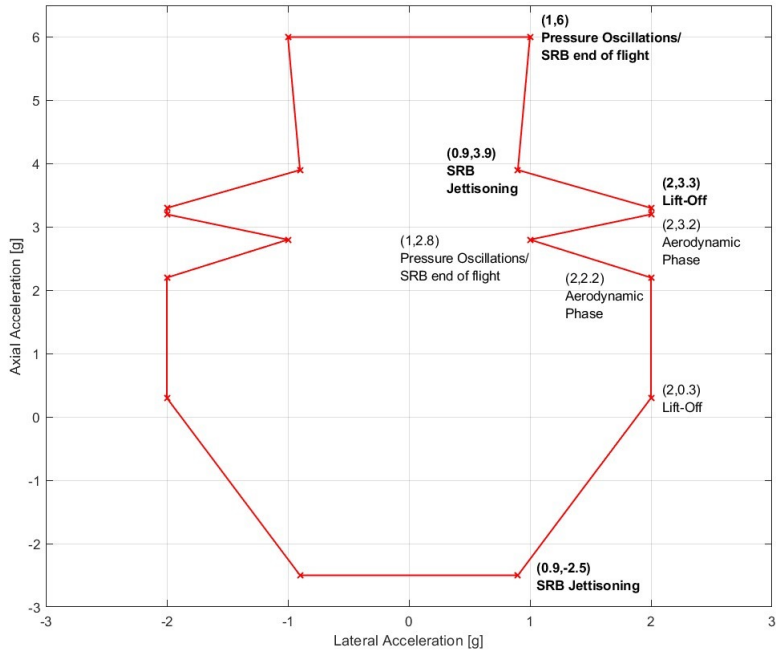


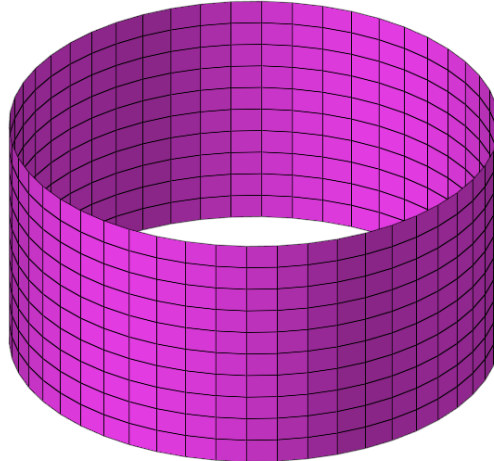
Figure 9: Envelope Quasi-Static Loads – Flight limit levels - Design Load Factors.

The visual and practical aspect of this envelope is that the acceleration limits of the worst possible combinations are at the corners, so the [QSLs](#) of the launch will stay within this envelope. This is why it is much more practical to perform the quasistatic analysis at each point of the envelope, which in this case would translate into 8 subcases or [CFEs](#) (16 if the symmetrical ones are counted). It is also necessary to consider that out of these 8 [CFEs](#), there are 4 with the same lateral acceleration but different axial accelerations. In this case, the [CFEs](#) with the highest axial acceleration would be more structurally demanding than the other 3, making the analysis of these other 3 [CFEs](#) unnecessary. The same logic applies to the [CFE](#) (1;2.8) “Pressure Oscillations/SRB end of flight”, so the 4 [CFEs](#) to be considered are those indicated in bold in the previous [Figure 9](#).

5.2 Aluminum interstage structure

For the first iteration, a structure made entirely of aluminum was created. A cylinder with the general dimensions of the Ariane 5 interstage structure was designed in CATIA V5 (see [Table 3](#) for general dimensions). This model was then imported into HyperMesh. Before creating the mesh, it was considered that a 3D mesh was not necessary for this type of structure. A mesh like the one shown in the following [Figure 10](#), which represents a cylindrical surface, was deemed sufficient. In this case, the cylindrical surface was created using the “middle surface” command in HyperMesh.

Total Height	Diameter
2759 mm	5437 mm

Table 3: General dimensions ISS Ariane 5**Figure 10:** Cylindrical mesh interstage structure.

After creating the mesh, the material was selected: an aluminum 7050 with a Young's modulus of 75,000 MPa, a Poisson's ratio of 0.33, and a density of 2.7e-9 tons, as discussed in subsection 3.3

To clarify, every time data with units is mentioned, the specific units used will be indicated to ensure the dimensional analysis is consistent. Refer to the following Figure 11 to see the units applicable for this system, which in this case are [mm/N/MPa].

System of Units	Input								Output		
	Length	Force	Elastic Modulus	Mass	Mass Density	WTMASS Param	Acceleration (1 G)		Disp	Force	Stress
1 Metric meter-kg	m	N	Pa	kg	Kg/m ³	1.0	9.807	m/sec ²	m	N	Pa
2 Metric mm-ton	mm	N	MPa	t or Mg	t/mm ³ or Mg/mm ³	1.0	9807	mm/sec ²	mm	N	MPa
3 English ft-lb	ft	lbf	psf	slug	slug/ft ³	1.0	32.17	ft/sec ²	ft	lbf	psf
4 English in-lb (mass)	in	lbf	psi	lbf - sec ² /in	lbf - sec ² /in ⁴	1.0	386.1	in/sec ²	in	lbf	psi
5 English in-lb (force)	in	lbf	psi	lbf	lbf/in ³	0.00259	386.1	in/sec ²	in	lbf	psi

Figure 11: Example of Consistant Systems of Units for Structural Analysis.

Next, a property was added to the material. Since the mesh is a surface, the property applied is PSHELL, which allows for adjustments in the thickness of the structure. For the first iteration, a thickness of 20 mm (which is excessive) was chosen. This initial thickness

is arbitrary because the objective is to gradually reduce it until the Margins of Safety are no longer positive, indicating that the structure is not strong enough.

For the Load Collector, Single Point Constraints were added for simplicity with HyperMesh. These constraints were applied to the lower circumference of the cylinder, as shown in the following [Figure 12](#). "123456" indicates that the node is constrained in all six degrees of freedom.

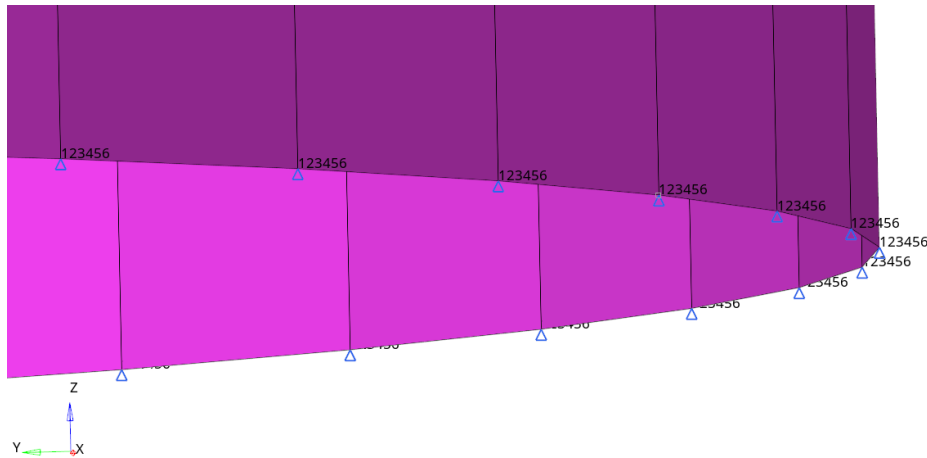


Figure 12: SPCs at interstage base.

Up to this point, it is recommended to use HyperMesh to create the “model data”. This file is available on GitHub as a .h file. The next step is to export it as a .bdf (bulk data file), which is also available on GitHub. The export file type is NASTRAN, as the analyses were conducted using NASTRAN. This exported file has been briefly modified, and a .dat file was created. However, the .bdf file can remain unchanged, allowing changes to the analysis or modifications to the loads in the .dat file. On the other hand, the .bdf can be refined, and once the .dat file of the analysis is complete, it can simply be run again to check the results without being changed. The .dat file dictates the analysis, loads, and different subcases, as explained below.

Here is an explanation of what a .dat file is and how its structure. The following [Figure 13](#) shows the typical structure of a .bdf file, which consists of three main sections:

1. **Executive Control Deck:** Specifies the type of solution and optionally sets a time limit for the process.
2. **Case Control Deck:** Determines which sub-case to calculate, assigns a title, selects load collectors to the subcase (SPCs and LOADs), and specifies which plots to generate.
3. **Bulk Data Deck:** Contains all the model data and specifies the LOADS and GRAV cards for the different subcases.

Keep in mind that while this explanation is for a complete BDF, in practice, the data is usually split into two or more files: the BDFs and the .dat. The .dat file runs the analysis.

In the Bulk Data Deck of the .dat, the necessary BDFs are imported or “included”. In this first case, only one model is included, but multiple BDFs can be included in this Deck. For a better understanding, refer to “QSL_interstage_Subcases.dat” on GitHub.

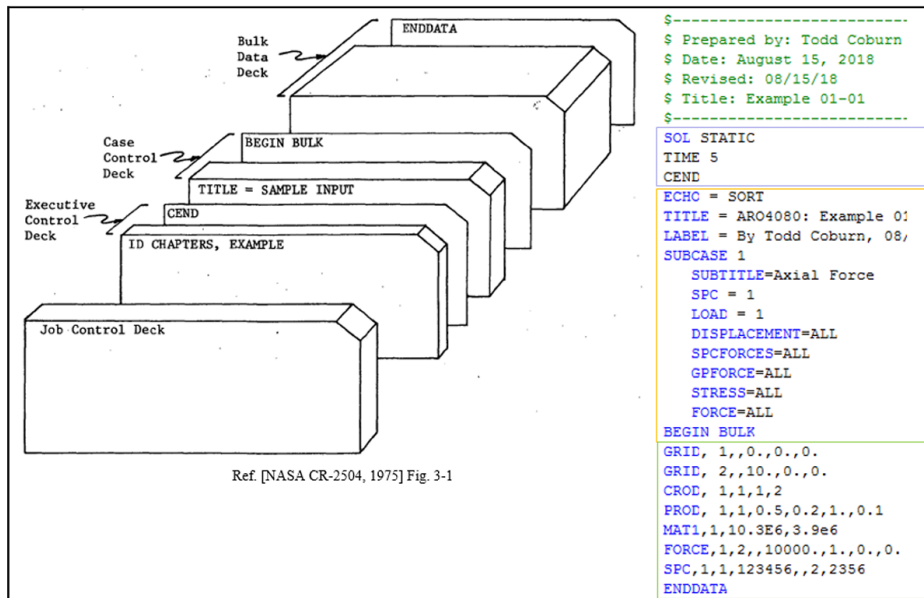


Figure 13: Basic Format of NASTRAN Bulk Data File (BDF).

subsubsection 5.2.1 provides a detailed explanation of the created cards and the criteria used for their creation.

5.2.1 Aluminum QSL Analysis

For the quasi-static analysis of the interstage structure, the 4 CFEs discussed in subsection 5.1 (indicated in bold in Figure 9) have been analyzed. Each CFE has been converted into 12 subcases by rotating the lateral acceleration every 30 deg. This approach is taken because there is no certainty about the direction of this acceleration—it could be along the x-axis, y-axis, or a combination of both from the launcher. Therefore, for structures that are not symmetrical, the lateral acceleration is rotated to analyze all possible lateral directions.

Until now, the structure has been completely symmetrical, but the objective is to make some modifications, such as adding windows or components, which could alter the results. In such cases, without rotation, potential weak points might not be detected. In practice, even finer rotations, such as 15 degrees or less, are often used to ensure comprehensive analysis.

The following Figure 14 corresponds to the 12 subcases resulting from the first CFE at Lift-Off. It also shows the gravity cards introducing the axial acceleration in the z-axis and the lateral acceleration in the x- and y-axes, rotating every 30 degrees. Note that the axial acceleration is not 3.3g. Instead, it is 3.3g multiplied by a safety factor (1.25), resulting in 4.125g. This adjustment is necessary because, according to the safety factors outlined in the User’s Manual, the accelerations must be scaled for qualification models as already discussed in subsubsection 3.2.1.

<u>## CFE_1 - LIFT-OFF</u>					
SUBCASE 101	SUBCASE 107	LOAD	101	1.0	1.0 1101
LABEL=QSL_101	LABEL=QSL_107	LOAD	102	1.0	1.0 1102
SPC=1	SPC=1	LOAD	103	1.0	1.0 1103
LOAD=101	LOAD=107	LOAD	104	1.0	1.0 1104
		LOAD	105	1.0	1.0 1105
SUBCASE 102	SUBCASE 108	LOAD	106	1.0	1.0 1106
LABEL=QSL_102	LABEL=QSL_108	LOAD	107	1.0	1.0 1107
SPC=1	SPC=1	LOAD	108	1.0	1.0 1108
LOAD=102	LOAD=108	LOAD	109	1.0	1.0 1109
		LOAD	110	1.0	1.0 1110
SUBCASE 103	SUBCASE 109	LOAD	111	1.0	1.0 1111
LABEL=QSL_103	LABEL=QSL_109	LOAD	112	1.0	1.0 1112
<u>## CFE_1 - LIFT-OFF</u>					
SPC=1	LOAD=109	GRAV	1101	-9810.	2.5000 0.0000 4.1250
SUBCASE 104	SUBCASE 110	GRAV	1102	-9810.	2.1651 1.2500 4.1250
SPC=1	LABEL=QSL_110	GRAV	1103	-9810.	1.2500 2.1651 4.1250
LOAD=104	SPC=1	GRAV	1104	-9810.	0.0000 2.5000 4.1250
	LOAD=110	GRAV	1105	-9810.	-1.2500 2.1651 4.1250
SUBCASE 105	SUBCASE 111	GRAV	1106	-9810.	-2.1651 1.2500 4.1250
LABEL=QSL_105	LABEL=QSL_111	GRAV	1107	-9810.	-2.5000 0.0000 4.1250
SPC=1	SPC=1	GRAV	1108	-9810.	-2.1651 -1.2500 4.1250
LOAD=105	LOAD=111	GRAV	1109	-9810.	-1.2500 -2.1651 4.1250
		GRAV	1110	-9810.	0.0000 -2.5000 4.1250
SUBCASE 106	SUBCASE 112	GRAV	1111	-9810.	1.2500 -2.1651 4.1250
LABEL=QSL_106	LABEL=QSL_112	GRAV	1112	-9810.	2.1651 -1.2500 4.1250
SPC=1	SPC=1				
LOAD=106	LOAD=112				

Figure 14: Definition of subcases and cards in .dat file for the Lift-Off CFE.

5.2.1.1 Upper stage axial and shear stress contribution

Up to this point, only the accelerations experienced by the interstage structure have been considered (by its own mass). However, additional forces involved in the launch must be taken into account. Firstly, on top of this interstage is the upper stage, also called ESC-A. According to the User's Manual, [Figure 15](#), and various sources such as reference [17], the estimated total weight of the upper stage is 42,850 kg. The following [Table 4](#) shows the different weights and the total sum of the upper stage ESC-A. Worst configurations have been considered.

PAYOUT FAIRING		CRYOGENIC UPPER STAGE (ESC-A)	
Diameter	5.4 m	Size	$\varnothing 5.4 \text{ m} \times 4.711 \text{ m}$ between I/F rings
Height	17 m	Dry mass	4540 kg
Mass	2675 kg	Structure	Aluminium alloy tanks
Structure	Two halves - Sandwich CFRP sheets and aluminium honeycomb core	Propulsion	HMTB engine - 1 chamber
Acoustic protection	Foam sheets	Propellants loaded	14.9 t of LOX + LH ₂
Separation	Horizontal and vertical separations by leak-proof pyrotechnical expanding tubes	Thrust	67 kN
SYLDAS		Isp	446 s
Diameter	4.56 m	Feed system	1 turbo-pump driven by a gas generator
Height	Total height of standard version: 4.903 m	Pressurization	GHe for LOX tank and GH ₂ for LH ₂ tank
	Adjustable cylinder height : +0.3/+0.6/+0.9/+1.2/+1.5/+2.1 m w.r.t. standard	Combustion time	945 s
Mass	From 425 to 535 kg, depending on height	Attitude control	Pitch and yaw: gimballed nozzle
Structure	Sandwich CFRP sheets and aluminium honeycomb core	powered phase	Roll: 4 GH ₂ thrusters
Separation	Leak-proof pyrotechnical expanding tube at the base of the cylinder	Attitude control	Roll, pitch and yaw : 4 clusters of 3 GH ₂ thrusters
ADAPTERS		ballistic phase	Longitudinal boost : 2 GO ₂ thrusters
Clampband	$\varnothing 937 \ 01194 \ \varnothing 1666 \ \varnothing 2624$	Avionics	Guidance from VEB
4 pyronuts	$\varnothing 1663$	INTER STAGE STRUCTURE (ISS)	
CONE 3936 or LVA 3936		Structure	Sandwich CFRP sheets and aluminium honeycomb core
Height	783 or 1187 mm	Separation	Pyrotechnical expanding tube at the top of the ISS and 4 ullage rockets
Mass	200 or 170 kg	CRYOGENIC MAIN CORE STAGE (EPC)	
Structure	Monolithic CFRP cone and glass fiber membrane	Size	$\varnothing 5.4 \text{ m} \times 23.8 \text{ m}$ (without engine)
VEB		Dry mass	14700 kg
Structure	Sandwich CFRP sheets and aluminium honeycomb core	Structure	Aluminium alloy tanks
Avionics	Flight control, flight termination, power distribution and telemetry subsystems	Propulsion	Vulcain 2 - 1 chamber
SOLID ROCKET BOOSTER (EAP)		Propellants	170 t of LOX + LH ₂
		Thrust	960 kN (SL) 1390 kN (Vacuum)
		Isp	$\sim 310 \text{ s (SL)} \ 432 \text{ s (Vacuum)}$
		Feed system	2 turbo-pumps driven by a gas generator
		Pressurization	GHe for LOX tank and GH ₂ for LH ₂ tank
		Combustion time	540 s
		Attitude control	Pitch and yaw: gimballed nozzle
		Avionics	Roll: 4 GH ₂ thrusters
			Flight control, flight termination, power distribution and telemetry subsystems, connected to VEB via data bus

Figure 15: Launch vehicle general data, [1].

	ESC-A (dry mass+prop)	Fairing	Sylda 5	LVA	Payload	TOTAL
Mass [tons]	$4.54 + 14.9$	2.675	0.535	0.2	20	42.85

Table 4: ESC-A upper stage mass breakdown, [1].

In the same way, this total mass is multiplied by a safety factor of 1.25, resulting in 53.5625 tons to be considered for the analysis. To introduce this load, a spider or RBE2 (Rigid Body) element connects all the nodes of the upper circumference to a central node. This central node is where the external loads are applied. The following [Figure 16](#) illustrates this setup.

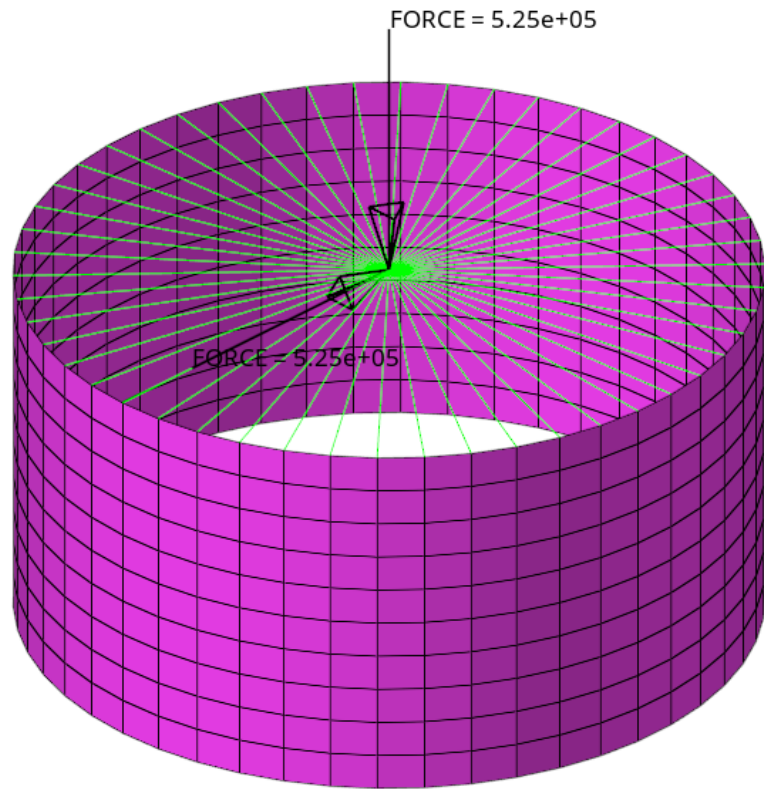


Figure 16: Example with RBE2 and vertical and shear forces.

As these are forces, they must be introduced in Newtons. Therefore, the total mass of the upper stage has to be multiplied by the G's it experiences in that direction. For example, in the first CFE Lift-Off, it has an axial acceleration of 3.3G's, which, when multiplied by 1.25, results in 4.125g. The calculation is as follows: $53562.5 \text{ kg} * 4.125 * 9.81 \text{ N/kg} = 2.167e6 \text{ N}$. This can be seen in the [Figure 17](#) of the vertical and shear forces below. Note that these forces align with the direction of the accelerations, rotating in the same manner—12 turns of 30 degrees with the same sign as the accelerations.

```
$> CFE_1 - LIFT-OFF; weight * axial/lateral accelerations = 525448.125N * 4.125/2.5g
$--01-->--02-->--03-->--04-->--05-->--06-->--07-->--08-->--09-->
FORCE    11101      551      0      1.0   -1.314+6      0.0   -2.167+6
FORCE    11102      551      0      1.0   -1.138+6-6.568+5-2.167+6
FORCE    11103      551      0      1.0   -6.568+5-1.138+6-2.167+6
FORCE    11104      551      0      1.0      0.0   -1.314+6-2.167+6
FORCE    11105      551      0      1.0   6.5681+5-1.138+6-2.167+6
FORCE    11106      551      0      1.0   1.1376+6-6.568+5-2.167+6
FORCE    11107      551      0      1.0   1.3136+6      0.0   -2.167+6
FORCE    11108      551      0      1.0   1.1376+66.5681+5-2.167+6
FORCE    11109      551      0      1.0   6.5681+51.1376+6-2.167+6
FORCE    11110      551      0      1.0      0.0   1.3136+6-2.167+6
FORCE    11111      551      0      1.0   -6.568+51.1376+6-2.167+6
FORCE    11112      551      0      1.0   -1.138+66.5681+5-2.167+6
```

Figure 17: Upper stage axial and shear forces.

5.2.1.2 Bending moment launcher contribution

Last but not least, it is necessary to consider another aspect of the launcher's dynamics: the bending moment created in flight by the forces from the axial and lateral accelerations acting on the launcher's center of gravity. This force, generated at the center of gravity, creates a moment due to the distance to the interstage/upper stage interface, which must be accounted for. According to calculations, this moment is one of the major contributors to the stresses on the structure.

To simplify the analysis, let's assume the launcher always maintains a zero angle of attack and the center of mass is always on the z-axis of the launcher. This assumption allows us to consider that the contribution of the axial acceleration to creating a moment at our interface is zero.

On the other hand, the contribution of lateral accelerations does create a moment. To calculate this, it is necessary to determine the center of gravity of the launcher at each moment and run multiple cases. This detailed analysis has not been performed here. Instead, the worst possible cases for both forces and center of mass position have been selected for each Critical Flight Event.

To determine the location of the center of mass, a model of the Ariane 5 has been created using the weights and dimensions specified in the "Launch Vehicle General Data" section of the User's Manual [Figure 18](#). The masses are approximate and represent the worst-case scenario. They are divided into three sections: the upper stage, main stage, and SRBs.



Figure 18: Ariane 5 CATIA model for masses distribution.

For the first Critical Flight Event, Lift-off, the total mass of the launcher before launch has been considered using the data from [Figure 15](#). This results in a mass of 707,550 kg, distributed according to the dimensions stated in the User's Manual. This distribution is approximate. According to online sources, the maximum weight the rocket can have at lift-off is 780 tons, leaving about 70 tons unaccounted for. Therefore, a safety margin of 1.25 has been applied.

With these 884.4 tons, the lateral force created by the lateral acceleration at lift-off can be calculated. In this case, it is $2g * 1.25$. This force is then multiplied by the distance

to the interstage/upper stage interface, which has been estimated by the CATIA model to be about 17.06 meters. Note that this distance increases as the launcher ascends, but the mass of the launcher decreases, requiring multiple cases to determine if this momentum is increasing, decreasing, or remaining stable. To simplify, this distance has been multiplied by a higher safety factor of 1.5, ensuring that the calculated condition is very demanding and will not be exceeded. Having accurate information, the exact position of the center of gravity throughout the launch, and sufficient time would allow for a more precise calculation of the momentum generated at the interface, preventing over-dimensioning of the interstage.

For the second Critical Flight Event (CFE), Pressure Oscillations/SRB End of Flight, the dry mass of the empty Solid Rocket Boosters (SRBs) has been considered negligible compared to the 240 tons of SRB propellant. Therefore, this CFE is approximately similar to CFE3 and CFE4, SRB Jettisoning.

For the calculation of the lateral force and the center of gravity (CoG) position during the second Critical Flight Event (CFE), Pressure Oscillations/SRB End of Flight, the mass of the main and upper stage is considered. The cards and the values of the moment calculations for the first critical flight event, Lift-Off, are shown in [Figure 19](#). Note that these moments must align with the direction of the accelerations, so the signs will vary accordingly.

```
$$ CFE_1 - LIFT-OFF; T = (weight * axial_acc*SF)*distance*SF = (707550kg*1.25 * 2g*1.25)*17060mm*1.5
$--01-->--02--><--03--><--04--><--05--><--06--><--07--><--08--><--09-->
MOMENT 111101 551 0 1.0 0.0 -5.55+11 0.0
MOMENT 111102 551 0 1.0 2.775+11-4.81+11 0.0
MOMENT 111103 551 0 1.0 4.807+11-2.78+11 0.0
MOMENT 111104 551 0 1.0 5.551+11 0.0 0.0
MOMENT 111105 551 0 1.0 4.807+112.775+11 0.0
MOMENT 111106 551 0 1.0 2.775+114.807+11 0.0
MOMENT 111107 551 0 1.0 0.0 5.551+11 0.0
MOMENT 111108 551 0 1.0 -2.78+114.807+11 0.0
MOMENT 111109 551 0 1.0 -4.81+112.775+11 0.0
MOMENT 111110 551 0 1.0 -5.55+11 0.0 0.0
MOMENT 111111 551 0 1.0 -4.81+11-2.78+11 0.0
MOMENT 111112 551 0 1.0 -2.78+11-4.81+11 0.0
```

Figure 19: Momentum cards definition for Lift-Off CFE.

5.2.2 Aluminum QSL Results

The following [Figure 20](#) shows the maximum stresses experienced by the interstage across all subcases. This includes the worst stresses from the 4 critical flight events (CFEs), with each CFE having 12 subcases due to rotations. As mentioned earlier, the primary contributor to these stresses is the bending moment. This result is for a single cylinder with a thickness of 20mm of Aluminum 7050, weighing approximately 2.5 tons.

As observed, the highest stress is 1316 MPa. Given that the yield stress of aluminum is 455 MPa, this stress level significantly exceeds the allowable limit and does not give us a positive Margin of Safety as already defined in [Equation 1](#).

To ensure a safety margin, the cylinder thickness should be at least 76 mm, resulting in a maximum stress of 360.3 MPa and a Margin of Safety (MoS) of 0.01, as shown in [Figure 21](#).

This configuration weighs 9.66 tons, which is far too heavy. There is still much room for improvement. The buckling results will require higher stiffness, so the thickness will need to be increased to prevent the structure from collapsing under compression. The goal is to

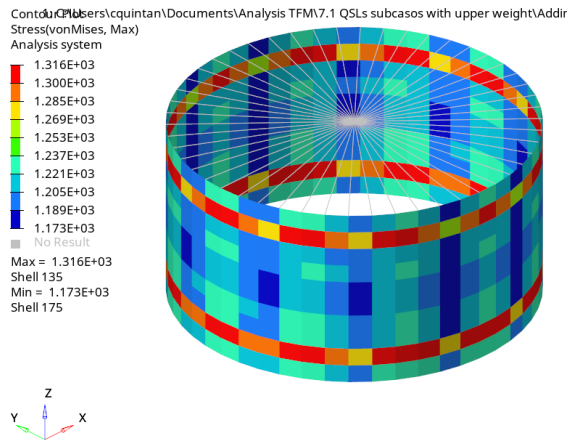


Figure 20: QSL stresses for Aluminum, thickness = 20mm.

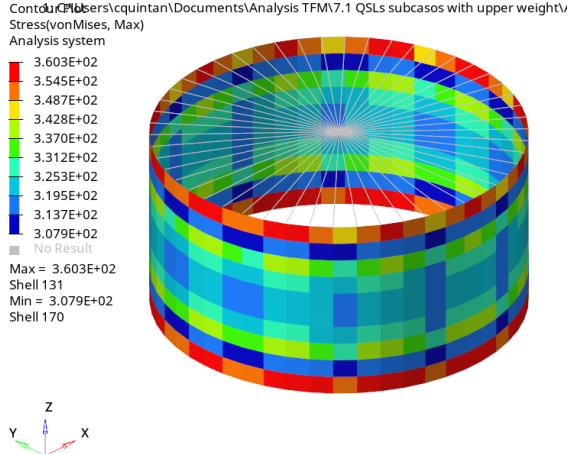


Figure 21: QSL stresses for Aluminum, thickness = 76mm.

demonstrate the process from the simplest configuration—a cylinder—to more complex designs. Later sections will explain the transition from solid material to honeycomb structures and compare the improvements. Following this, the integration of upper and lower rings, as well as frames and stringers, will be discussed to enhance the structure’s thickness and weight efficiency.

5.2.3 Aluminum Buckling Analysis

For the buckling analysis of the interstage structure, only 3 of the 4 CFEs discussed in subsection 5.1 (indicated in bold in Figure 9) have been analyzed. The SRB jettisoning 2 event involves tension, making buckling analysis unnecessary.

Each CFE has been converted into 12 subcases by rotating the lateral acceleration every 30 deg as mentioned before. The 12 subcases for each CFE remain the same, with identical GRAV and LOAD cards, as shown in Figure 14. However, buckling subcases are now added. Figure 22 displays the typical structure for the buckling subcases for the Lift-Off CFE. Each of these subcases considers the corresponding static conditions, with the STATSUB card referencing the specific subcase.

SS CFE 1 - LIFT-OFF - BUCKLING

SUBCASE 1010 LABEL=1010_ULTIMATE-LOAD_BUCKLING METHOD=12 STATSUB=101 SPC=1 DISPLACEMENT=ALL SPCFORCES=ALL SVECTOR=ALL	SUBCASE 1050 LABEL=1050_ULTIMATE-LOAD_BUCKLING METHOD=12 STATSUB=105 SPC=1 DISPLACEMENT=ALL SPCFORCES=ALL SVECTOR=ALL	SUBCASE 1090 LABEL=1090_ULTIMATE-LOAD_BUCKLING METHOD=12 STATSUB=109 SPC=1 DISPLACEMENT=ALL SPCFORCES=ALL SVECTOR=ALL
SUBCASE 1020 LABEL=1020_ULTIMATE-LOAD_BUCKLING METHOD=12 STATSUB=102 SPC=1 DISPLACEMENT=ALL SPCFORCES=ALL SVECTOR=ALL	SUBCASE 1060 LABEL=1060_ULTIMATE-LOAD_BUCKLING METHOD=12 STATSUB=106 SPC=1 DISPLACEMENT=ALL SPCFORCES=ALL SVECTOR=ALL	SUBCASE 1100 LABEL=1010_ULTIMATE-LOAD_BUCKLING METHOD=12 STATSUB=110 SPC=1 DISPLACEMENT=ALL SPCFORCES=ALL SVECTOR=ALL
SUBCASE 1030 LABEL=1030_ULTIMATE-LOAD_BUCKLING METHOD=12	SUBCASE 1070 LABEL=1070_ULTIMATE-LOAD_BUCKLING METHOD=12	SUBCASE 1110 LABEL=1110_ULTIMATE-LOAD_BUCKLING METHOD=12

Figure 22: Definition of buckling subcases in .dat file for the Lift-Off [CFE](#).

When the bending moment is added to the analysis, some negative values symmetrical to the positive ones appear in the results. This could be due to several reasons, but since it only occurs when introducing this stress, it is likely a behavior of the software itself rather than representing real values.

5.2.4 Aluminum Buckling Results

At 76 mm, the case exhibits a positive buckling margin. To determine the Margin of Safety (MoS) for buckling, the following [Equation 2](#) is utilized, which is essentially the same as the one previously mentioned but expressed differently, [Equation 1](#). Lambda represents the minimum eigenvalue, while K_{DF} stands for the known down factor.

$$BMoS = \frac{\lambda \cdot K_{DF}}{SF} - 1 > 0 \quad (2)$$

Lambda represents a load factor, calculated as $\lambda = \sigma_{allowable}/\sigma_{applied}$, and K_{DF} Known Down Factor or Buckling Factor. Considers factors like material imperfections, geometric deflections, and load misalignments that may affect a structure's buckling resistance. It adjusts the theoretical buckling resistance to a more conservative value. Typically, for cylinders, values range between 0.66 and 0.5. For this case, 0.5 is used to ensure a more conservative approach.

For the 76 mm case, the first eigenvalue is 4.752, which translates into a Buckling Margin of Safety (BMOS) of 0.9, indicating a positive margin. Therefore, 76 mm would be the thickness that satisfies both the Quasi-Static Loads (QSL) and buckling analysis requirements for a 7075 Aluminum structure, with a weight of 9.66 tons.

5.3 Honeycomb Interstage Structure

For this case, the only change compared to the aluminum case is the material, see [subsection 5.2](#). Instead of using aluminum, a honeycomb structure with an aluminum core and CFRP skins has been selected. The aluminum properties remain as described above in [subsubsection 3.3.1](#), and the CFRP properties are initially as outlined in [Table 2](#).

However, during the analysis of the results, it has been observed that CFRP is quite flexible and can have its stiffness or maximum stress adjusted as needed. This capability was not available with aluminum, making it the limiting factor in the quasi-static analysis with respect to buckling.

In the iterative process of this example explained below, a structure of 7.67 tons has been achieved with a thickness of 53 mm for the aluminum core and 6 mm for the skin, 65 mm in total. This is 10 mm less than the aluminum case, but the main advantage over the aluminum case is that it is 2 tons lighter. The following [Table 5](#) shows a comparison of the two cases.

	Thickness [mm]	Weight [tons]
Aluminum case	76	9.66
Honeycomb case	65	7.67

Table 5: Comparison of thicknesses and weights of the two case studies.

It should be noted that these thickness results are too large, but they will be reduced when stiffeners such as frames and stringers are added. However, for this case, only the cylindrical structure has been considered, as in the previous case, so the trade-off between stiffness and stress has been done accordingly.

5.3.1 Honeycomb QSL and Buckling Analysis

Therefore, in this iterative process, the aim was to obtain a skin thickness between 2 and 6 mm. A typical value for each ply in CFRP is 0.2 mm. Selecting a skin thickness of 4 mm results in 20 plies. The arrangement of the fibers depends on the conditions in which the material needs to be enhanced. In this case, the problem has been simplified by creating an isotropic skin, with the layers oriented in all directions and interspersed at about 90 degrees to each other.

The final orientation of a 20-ply skin is as follows: [0/90/45/-45/9/-81/81/-9/36/-54/72/-18/27/-63/54/-36/18/-72/63/-27], as shown in the following [Figure 23](#).

```
$--01-->--02-->--03-->--04-->--05-->--06-->--07-->--08-->--09-->
PCOMP    2      0.0
          1     0.3   0.0    YES    1     0.3   90.0   YES
          1     0.3   45.0   YES    1     0.3  -45.0   YES
          1     0.3    9.0    YES    1     0.3  -81.0   YES
          1     0.3   81.0    YES    1     0.3   -9.0   YES
          1     0.3   36.0    YES    1     0.3  -54.0   YES
          1     0.3   72.0    YES    1     0.3  -18.0   YES
          1     0.3   27.0    YES    1     0.3  -63.0   YES
          1     0.3   54.0    YES    1     0.3  -36.0   YES
          1     0.3   18.0    YES    1     0.3  -72.0   YES
          1     0.3   63.0    YES    1     0.3  -27.0   YES
          3     53.0   0.0    YES    1     0.3   90.0   YES
          1     0.3   0.0    YES    1     0.3   90.0   YES
          1     0.3   45.0    YES    1     0.3  -45.0   YES
          1     0.3    9.0    YES    1     0.3  -81.0   YES
          1     0.3   81.0    YES    1     0.3   -9.0   YES
          1     0.3   36.0    YES    1     0.3  -54.0   YES
          1     0.3   72.0    YES    1     0.3  -18.0   YES
          1     0.3   27.0    YES    1     0.3  -63.0   YES
          1     0.3   54.0    YES    1     0.3  -36.0   YES
          1     0.3   18.0    YES    1     0.3  -72.0   YES
          1     0.3   63.0    YES    1     0.3  -27.0   YES
```

Figure 23: Definition PCOMP card .bdf for the Honeycomb case.

With such a structure, as in the aluminum case, the quasistatic case is the limiting one. The properties of the CFRP have been modified to adjust the stiffness and strength values accordingly. In the buckling analyses, there was too much margin, indicating that the structure was too stiff. Therefore, the Young's modulus values of the CFRP have been reduced, decreasing the stiffness and, consequently, the stress. With this margin, the thickness has also been adjusted to reach an equilibrium where the two analyses are close to the limit of safety margins.

In summary, for this case, the thickness of each CFRP ply has been increased from 0.2 mm to 0.3 mm, and the Young's modulus of the CFRP has been reduced to decrease the stiffness while increasing the stress resistance. See [Table 6](#) for CFRP properties applied for this case. And see [Figure 24](#) to see the the format used to describe these properties in the BDF.

E1	E2	NU12	G12	G1, Z	G2, Z
80 GPa	4 GPa	0.3	7 GPa	5 GPa	5 GPa
RHO	Xt	Xc	Yt	Yc	S
1600 kg/m ³	700 MPa	-700 MPa	600 MPa	-600 MPa	75 MPa

Table 6: Carbon Fiber Reinforced Polymer final properties.

```
$--01-->--02-->--03-->--04-->--05-->--06-->--07-->--08-->--09-->
MAT8      180000.0  4000.0  0.3      7000.0  5000.0  5000.0  1.6-9  +
+           700.0    700.0    600.0    600.0    75.0
```

Figure 24: Definition MAT8 card .bdf for the Honeycomb case.

Para facilitar el proceso iterativo se han calculado cuales son los margenes de seguridad MOS and BMOS, equation 1 and equation2, para este caso. Suponiendo un yield strenght para el CFRP de 700 MPa (orientative, see section material considerations to know more about

this) en la equation1, objetenemos que el estres maximo permitido seria de 560 MPa. Y para el BMOS el eigenvalue que necesitariamos seria de 2.5 minimo

To facilitate the iterative process, the MOS and BMOS have been calculated using [Equation 1](#) and [Equation 2](#). Assuming a yield stress for CFRP of 700 MPa (as an estimate, see the section on material considerations for more details), the maximum allowable stress using a SF of 1.25 would be 560 MPa. For BMOS, using a SF of 1.25 and a K_{DF} of 0.5 the minimum required eigenvalue is 2.5.

5.3.2 Honeycomb QSL Results

With the iterative process explained in the previous section, the following optimized result has been reached, as shown in [Figure 25](#). With a skin thickness of 6mm composed of 20 layers (0.3mm each) of CFRP, and a core of 53mm of aluminum, the maximum stress is 553 MPa. Considering a yield strength of 700 MPa, the safety margin calculated using [Equation 1](#) is positive, MoS = 0.013.

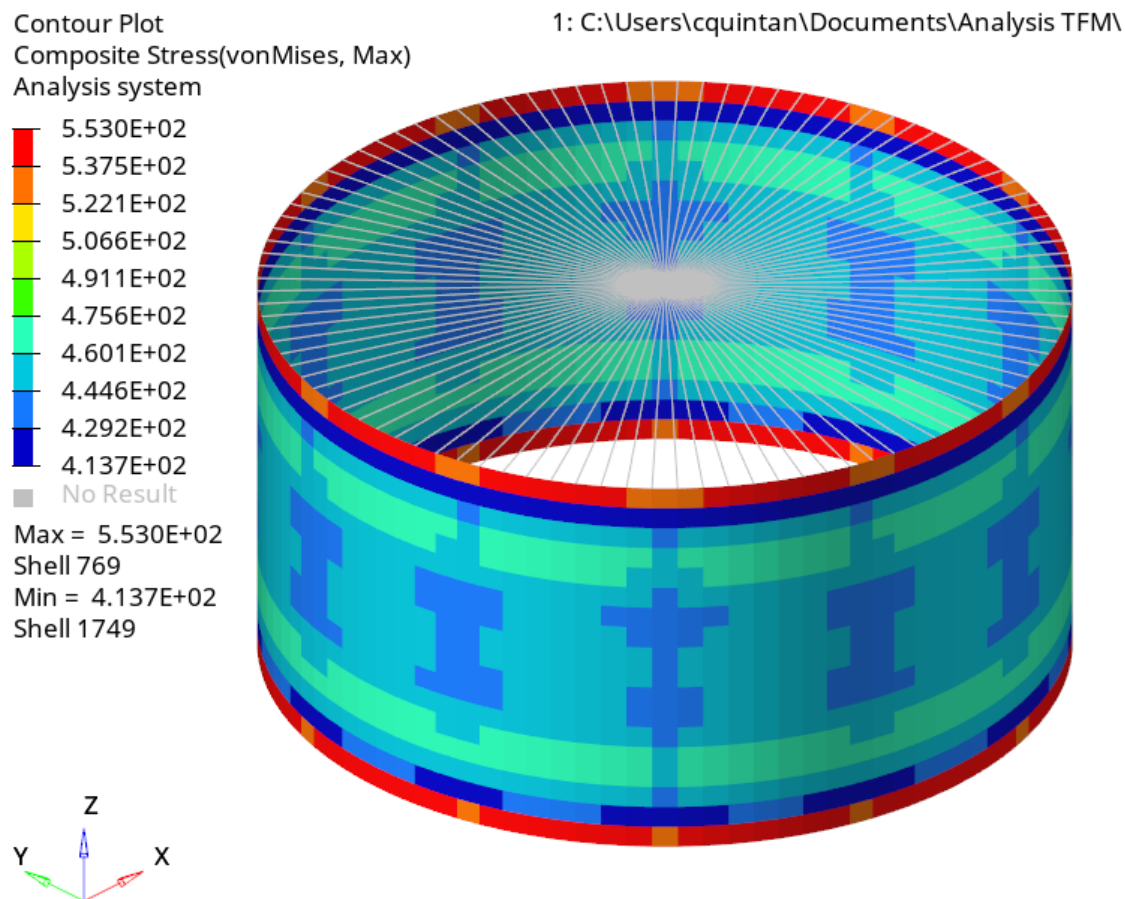


Figure 25: QSL optimized result Honeycomb case.

5.3.3 Honeycomb Buckling Results

With the same configuration as above after iteration, the lowest eigenvalue is 2.685 (the limit would be 2.5 as explained before). Using [Equation 2](#) and applying a safety factor (SF) of 1.25 and a K_{DF} of 0.5, a positive BMOS of 0.074 is obtained. By further adjusting the material properties and thickness, this problem could be optimized to bring both safety margins as close to zero as possible while minimizing the weight of the structure.

6 Design

6.1 Challenges

It is imperative to ensure that structural integrity is maintained consistently throughout all phases of the flight

Structural assessments can be challenging

- Designs and failure modes are complex
- Designed with low margins for weight savings
- Designs are subject to severe launch and ascent loads
- Hardware may not be perfect according to specifications due to defects, low material properties, not meeting tolerances, or others.

That is why it is required a fundamental understanding of the structural part, its function and failure modes

6.2 Failure Modes

6.2.1 System level failure modes

- Creep, strength, fatigue, fracture/fatigue, excessive yielding
- Corrosion, hydrogen embitterment

From those we are going to discard the chemical part and focus more in the structural limits, strength and creep

The source of many of these failure modes can be due to manufacturing errors, impact damage, excessive loads, etc.

6.3 Requirements analysis and mission profile considerations

El profile consideration que se ha considerado ha sido el fundamentalmente el profile quasistatic loads del manual de usuario como se puede ver en la siguiente imagen.

Los requisitos, los margenes de seguridad y MOS positivos COMO IREMOS VIENDO

6.4 Conceptual design phase

Requisitos dimensionales, altura, diametro... IF y cargas

7 Mechanical Environments

”Eso es, añadir la environmental spec, que viene en el manual del lanzador, es un documento con el que tendrás que familiarizarte, suelen estar disponibles online”

7.1 Structural loads and their effects?

7.2 Detailed design phase

7.3 Structural analysis and optimization techniques

8 Finite element description. Finite Element Analysis (FEA) techniques

”Se hace una breve descripción del FEM (geometría, malla, tipo de modelización, numeración...)”

9 Structural Analysis

9.1 Static Analysis

”Se puede añadir el free-free analysis (normal modes) para ver que todo está bien conectado”
Lo primero que se ha hecho es analizar nuestro cilindro simple para ver si cumplía MOS.

9.2 Buckling Analysis

9.3 Stress analysis and failure modes?

”Es parte del static analysis de buckling analysis, el obtener los márgenes de seguridad (MoS)” margins

10 Manufacturing and Testing

<https://headedforspace.com/how-rockets-are-made/>

10.1 Manufacturing techniques for interstage structures**10.2 Non-destructive testing methods****10.3 Full-scale testing and validation****11 Performance Evaluation****11.1 Comparative analysis of the designed interstage structure with existing ones****11.2 Evaluation of performance metrics such as weight, stiffness, and reliability****12 Future Developments and Challenges?****12.1 Emerging trends in launch vehicle design****12.2 Potential improvements in interstage structures****12.3 Challenges and areas for future research****13 Conclusion****14 References**

References

- [1] ArianeSpace. *Ariane 5 User's Manual*. chrome-extension://efaidnbmnnibpcajpcglclefindmkaj/https://www.arianespace.com/wp-content/uploads/2011/07/Ariane5_Users-Manual_October2016.pdf, 2016.
- [2] ArianeSpace. *Ariane 6 User's Manual*. chrome-extension://efaidnbmnnibpcajpcglclefindmkaj/https://www.arianespace.com/wp-content/uploads/2011/07/Ariane5_Users-Manual_October2016.pdf, 2021.
- [3] Richard Pantaleo Jaime Bourne. *Simulation of Launch Vehicle Dynamics on an Inter-stage Structure*. chrome-extension://efaidnbmnnibpcajpcglclefindmkaj/https://www.andrew.cmu.edu/user/rpantale/InterstageAnalysis_final.pdf, -.
- [4] JW Den Herder, AC Brinkman, SM Kahn, G Branduardi-Raymont, K Thomsen, H Aarts, M Audard, JV Bixler, AJ den Boggende, J Cottam, et al. The reflection grating spectrometer on board xmm-newton. *Astronomy & Astrophysics*, 365(1):L7–L17, 2001.
- [5] ESA. *THE EUROPEAN PHOTON IMAGING CAMERA (EPIC) ON-BOARD XMM-NEWTON*. <https://www.cosmos.esa.int/web/xmm-newton/technical-details-epic>, 2001.
- [6] ESA. *Ariane 5 Plus - Inter Stage Structure*. https://www.esa.int/ESA_Multimedia/Images/2001/11/Ariane_5_Plus_-_Inter.Stage_Structure, 2002.
- [7] ESA. *NASTRAN Handbook for ARO4080*. <chrome-extension://efaidnbmnnibpcajpcglclefindmkaj/https://toddcoburn.com/CPP/NASTRAN%20Handbook%20-%20Coburn%20-%2020181127.pdf>, 2002.
- [8] ESA. *Ariane 6 industrial organisation*. https://www.esa.int/ESA_Multimedia/Images/2016/11/Ariane_6_industrial_organisation, 2016.
- [9] ESA. *Vega-C 1/2 interstage integration CSG*. https://www.esa.int/ESA_Multimedia/Images/2022/04/C12i_interstage_integration_CSG, 2022.
- [10] Mssl Astrophysics Group. Images of the optical monitor. https://www.mssl.ucl.ac.uk/www_astro/xmm/om/OM_wheel.jpg.
- [11] JAXA. *About X-Ray Imaging and Spectroscopy Mission (XRISM)*. <https://global.jaxa.jp/projects/sas/xrism/>, 2019.
- [12] Steven M. Kahn, Jean Cottam, Todd A. Decker, Frits B. S. Paerels, Steven M. Pratuch, Andrew P. Rasmussen, Joshua Spodek, Jay V. Bixler, A. C. Brinkman, Jan-Willem den Herder, and Christian Erd. Reflection grating arrays for the Reflection Grating Spectrometer on board XMM. In Oswald H. W. Siegmund and Mark A. Gummin, editors, *EUV, X-Ray, and Gamma-Ray Instrumentation for Astronomy VII*, volume 2808, pages 450 – 462. International Society for Optics and Photonics, SPIE, 1996.

- [13] NTRS. *Structural Design of Ares V Interstage Composite Structure*. <https://ntrs.nasa.gov/citations/20110010308>, 2011.
- [14] Wessel Wessels. *The Main Parts Of A Rocket: What They Are How They Work*. <https://headedforspace.com/the-main-parts-of-a-rocket-what-they-are-how-they-work/>, 2024.
- [15] Wessel Wessels. *What Is A Rocket Interstage?* <https://headedforspace.com/what-is-a-rocket-interstage/>, 2024.
- [16] Wikipedia. *Aluminium alloy*. https://en.wikipedia.org/wiki/Aluminium_alloy, 2024.
- [17] Wikipedia. *Ariane 5*. https://fr.wikipedia.org/wiki/Ariane_5, 2024.
- [18] Wikipedia. *Launch vehicle*. https://en.wikipedia.org/wiki/Launch_vehicle, 2024.
- [19] COLUMBIA UNIVERSITY IN THE CITY OF NEW YORK. *Astronomy Astrophysics*. <https://www.astro.columbia.edu>.